

Single-Layer Broadband Endfire Antenna with High-Gain and Stable Beams Based on Spoof Surface Plasmon Polaritons

Huan JIANG, Xiang-yu CAO, Huan-huan YANG, Jun GAO, Liao-ri JI-DI

The Information and Navigation College of Air Force Engineering University, Xi'an, Shaanxi, 710077, China

1079824998@qq.com

Submitted October 13, 2021 / Accepted June 17, 2022 / Online first July 15, 2022

Abstract. A single-layer broadband endfire antenna with high-gain and stable beams based on the spoof surface plasmon polaritons (SSPPs) is proposed in this paper. The amplitude and phase of the surface wave are controlled by asymmetric protrusions on both sides. The anti-symmetric structure is added to balance the upper and lower electric fields while adjusting the impedance matching at the same time. Eventually, endfire radiation is generated with a stable beam to the free space within 5.25–7.94 GHz to form a relative bandwidth of 40.8%. The maximum achieved gain is 11.7 dBi at 7.1 GHz. The experimental results are basically consistent with the simulations. The antenna with high-gain, broadband and a stable beam can be effectively used in wireless communication systems.

Keywords

Spoof surface plasmon polaritons (SSPPs), endfire antennas, stable beams, broadband antennas

1. Introduction

Spoof Surface Plasmon Polaritons (SSPPs) can be generated on the dielectric-metal surface upon excitation of electromagnetic (EM) waves in the microwave range [1]. The proposed SSPPs can limit EM waves in the SSPPs transmission line (TL) to form a slow wave and realize the characteristics similar to SPP in the frequency range of light waves [2]. Many SSPPs functional devices can well meet the requirements of wireless communication networks [3], [4], among them, the SSPPs based antenna has received specific attention. The constraint of SSPPs on the surface wave is difficult to apply to the radiation of the antenna. In the follow-up studies, different kinds of matching structures have been shown to effectively match adopt both the surface wave and the free space wave, so as to break the field constraints of the field to achieve radiation [5].

It is difficult to design low-profile antennas without performance penalty, though the ultra-thin SSPP structures provide the possibility to fix a problem. The main task of

designing the single-layer endfire antenna is to form an asymmetric structure that may release the bounded SSPPs mode waves to the quasi-TEM mode since the symmetrical structure on both sides will lead to the formation of an anti-phase superposition at the end of the radiation, which makes it impossible to form an endfire effect at the end. In general, there are three ways to form an asymmetric structure. One method is to form an asymmetric feed structure, in which an asymmetric coplanar waveguide is used to form an asymmetric electric field to be guided by SSPPs TL and is radiated out through a graded groove structure. The second way is to form an asymmetric transmission structure. The electric field depends on different dispersion characteristics of the asymmetric SSPPs structure on both sides of a structure, which allows the synthesis of different phases and amplitudes of waves to be radiated into the space forming the endfire effect [6]. Another way is to form asymmetrical radiating parts. The asymmetric radiation structure is used to realize the endfire effect. With the elliptical radiators, the bandwidth is widened and the beam is pulled forward more steadily [7].

In this letter, we propose a single-layer endfire antenna based on SSPPs. The endfire antenna is designed with the control of amplitude and phase by the asymmetric SSPPs TL on both sides. Due to the current distribution of asymmetric structure, the antenna radiates at the endfire radiation plane while the maximum radiation direction deviates from the axis of the antenna in the entire operating bandwidth. To widen its bandwidth and enhance the stability of the beam as it varies with frequency, an improved endfire antenna design is proposed, in which the middle part of the mutation structure provides impedance matching and widens the bandwidth.

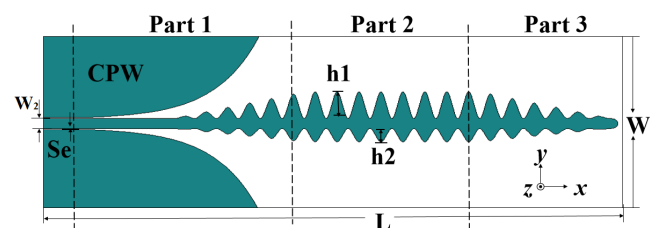


Fig. 1. The geometry of the proposed basic antenna.

2. Design of Basic Antenna

The proposed basic endfire antenna as shown in Fig. 1 is attached to a dielectric substrate with a dielectric constant of 2.65, a loss tangent equal to 0.003, and a thickness of 0.5 mm. The size of the substrate is $W \times L = 53.56 \text{ mm} \times 200 \text{ mm}$. The antenna is composed of three different functional parts.

Part 1 uses a coplanar waveguide (CPW) to feed. There is a microstrip line in the middle of CPW with the width of $W_2 = 3 \text{ mm}$, which is designed to match 50 Ω impedance of the subminiature SMA connector. The EM field is gradually bounded to the SSPPs mode by 6 mm-incremental structures. In addition, the gradient structure is beneficial to the transformation of free space wave mode and SSPPs wave mode. Conversion from quasi-TEM mode to SSPPs mode is achieved in part 1.

Part 2 consists of sinusoidal bulges of unequal height on both sides, $p = 5 \text{ mm}$, h_1 (on the upper side) = 7.4 mm, h_2 (on the lower side) = 4 mm. A total of 8 cycles are selected for the transmission part.

In part 3, the six-period tapering unit at the back end serves as the radiating part effectively radiating SPP mode into the free space. The periodic structure of the SSPP unit comprises series of sinusoidal bulges according to Fig. 2. The structure is only determined by the depth and period, which are easily controllable. In order to study the propagation characteristics of SSPP structure, we explore the dispersion relations using the Eigen-mode solver of the commercial software, CST Microwave Studio. Based on the dispersion characteristics of the SSPP unit structure, the higher the bump height is, the lower the cutoff frequency becomes. In order to adjust the endfire antenna operating bandwidth below 10 GHz, we have chosen the value of period $p = 5 \text{ mm}$, and sinusoidal amplitude $h = 7.4 \text{ mm}$, so that the cutoff frequency of the unit structure is around 8 GHz. Other antenna geometric parameters obtained after optimization in mm are as follows: $L_1 = 10$, $L_2 = 30$, $W_1 = 25$, $W_2 = 3$, $Se = 0.28$, $ln = 8.9$.

Gradient part extending from CPW to SSPPs TL enables at once mode conversion and impedance matching. The SSPPs TL can support the transmission of SSPPs mode waves, and gradually matches the energy bounded in the SSPPs TL with the free space waves through the gradient radiation part at the end of the antenna. Efficient impedance matching enables as little as possible energy to be reflected back to the free space so as to radiate into the free space. The influence of different h_1 on dispersion characteristics is shown in Fig. 2. It is obviously observed that the dispersion curve of this structure is below the light line forming slow waves on the interface. As the frequency increases the line approaches an asymptotic frequency and the wave vector increases sharply near the asymptotic frequency point. With the increase of the h_1 value, the dispersion curve gradually deviates from the light, the asymptotic frequency decreases significantly, and the ability to constrain surface waves of the structure gets enhanced. In our

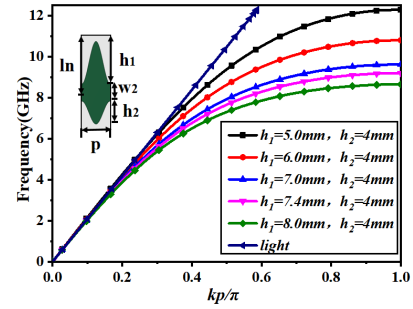


Fig. 2. Dispersion curve of the unit cell in SSPPs TL.

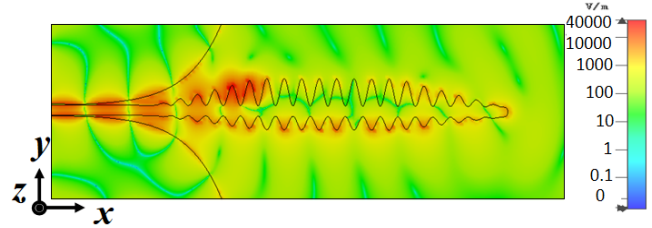


Fig. 3. The electric field intensity of the basic antenna at 10 GHz.

design ($h_1 = 7.4 \text{ mm}$), most of the energy can be transferred to the end. From the dispersion curve of the cells in Fig. 2, we can obtain that the cutoff frequency is 8.2 GHz.

To have the endfire effect, an asymmetric structure must be formed. The different height of the convex structure with different dispersion characteristics is used to construct sinusoidal convex on both sides of the microstrip line, forming the asymmetric structure to control SSPPs waves. It can be seen that most of the energy is still bounded between the antenna structures at 10 GHz, and ultimately the energy can hardly be radiated and is reflected back to the input end according to the electric field intensity of the basic antenna in Fig. 3.

The basic structure of the antenna is only composed of sinusoidal projections with different heights on both sides, as shown in Fig. 1. The near-field electric distribution is shown in Fig. 6(a). It can be seen that the EM wave guided by both sides of the transmission part at a given frequency points that the antenna produces different propagation phenomena within its operating bandwidth. The longer the sinusoidal protrusion structure is, the greater the phase velocity becomes and the faster the phase changes. Due to the current distribution of the asymmetric structure components, the radiation is carried out in the end-to-radiation plane, and the antenna can effectively radiate out in the range of 7.80–8.27 GHz. In Fig. 6, according to the electric field distribution of y components at 7.1 GHz, the field below is a half cycle longer than the field above, in addition to a 180 degrees phase difference generated by the transition part, so that the end of the antenna forms the end-to-radiate equiphase plane. Finally, under the guidance of the reduced part, transition from bounded SSPPs mode to radiating mode can be clearly observed. The electric field is constrained in the subwavelength structure by coupling with the components and propagating at the end of the antenna, forming an equiphase plane in free space.

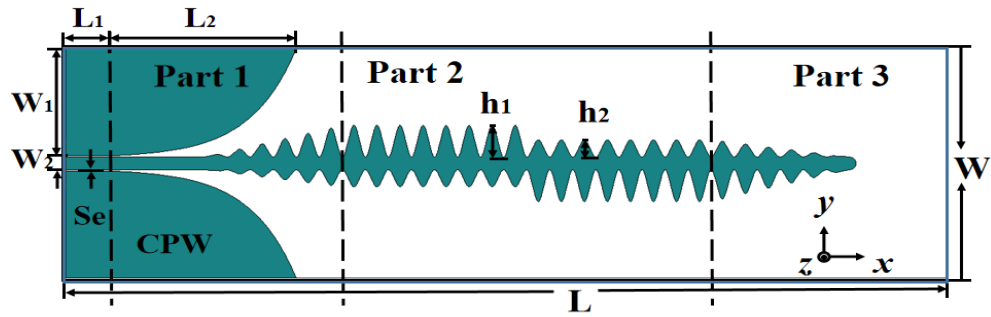


Fig. 4. The configuration of the improved SSPPs endfire antenna.

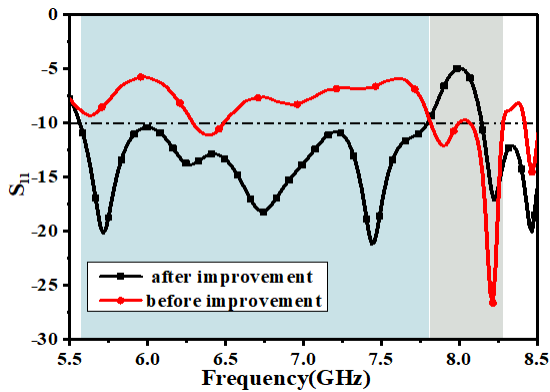


Fig. 5. Reflection's comparison of the endfire SSPPs antenna before and after the improvement.

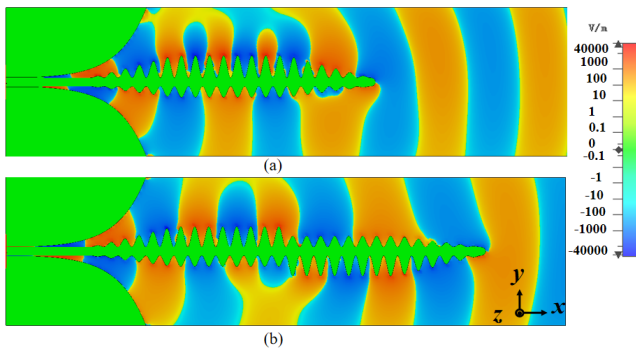


Fig. 6. Corresponding near-field distribution of y components. (a) Basic antenna at 8.2 GHz. (b) Improved antenna at 7.1 GHz.

Figure 7(a) shows the far-field orientation of the basic structure at 7.1 GHz. In addition, it is common that the maximum radiation direction deviates from the designed antenna axis and the deviation from the antenna axis is at least 8 degrees for the imbalance of electric field energy on both sides.

3. Design of Improved Antenna

To reduce this reflection, increase the bandwidth of the radiation, and enhance the frequency of the beam stabilization, an improved antenna is proposed as shown in Fig. 4. The improved structure compensates the electric field intensity of the front segment by reversing the electric field intensity of the back segment, so as to correct the end

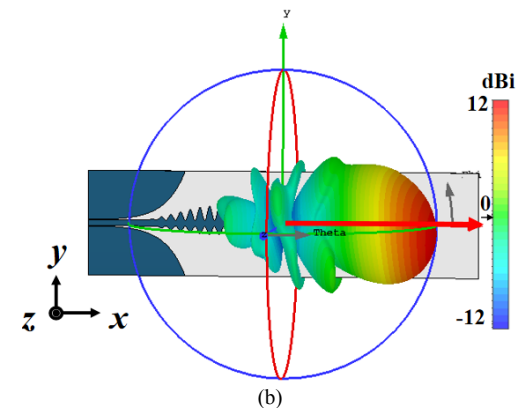
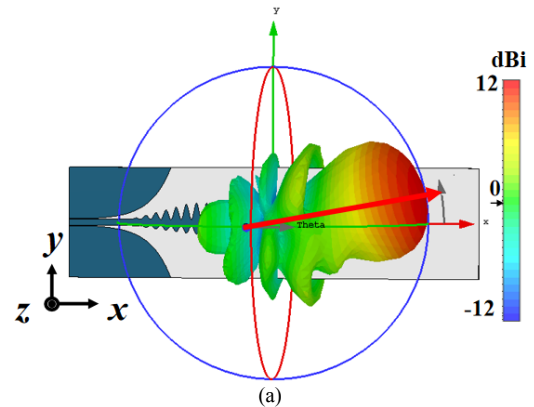


Fig. 7. Simulated far-field pattern of directivity. (a) Basic antenna at 8.2 GHz. (b) Improved antenna at 7.1 GHz.

radiating direction in the far-field. Then the antenna can achieve axial radiating of the antenna within the working bandwidth. The width of the upper and lower lateral protuberances is small, resulting in coupling between them, and it is this mutual coupling that extends the bandwidth to some extent. The far-field pattern of directivity in Fig. 7 shows that the overall beam of the improved structure is more consistent with the axis direction of the antenna. Compared to the basic model, the improved model exhibits narrower beam orientation, better directional orientation along the antenna axis, and wider bandwidth as shown in Fig. 5 and Fig. 7.

The end of the antenna can provide good phase matching to realize traveling waves and can well suppress reflection. In Fig. 5, the S_{11} curve suppressed below -10 dB of the improved antenna shows a wider bandwidth than the

basic one. Regarding the electric field distribution, the upper part of the front segment has strong constraint ability to EM, and the wave velocity is also slow. The transition from the segment with strong constraint ability to the segment with weak constraint ability in the back segment is relatively smooth. On the contrary, there will be a sudden change from the weak part to the strong one. Part of the energy cannot be transferred over, and it interacts with the original field in the form of radiation to achieve impedance matching and expand the bandwidth. The phase reversal property is generated at the mutation point, so that under the guidance of the rear end, the equiphase surface is formed at the end to produce the endfire effect. The lengthening of the anti-symmetric structure can increase the endfire gain to a certain extent. The relative bandwidth of the improved antenna is 40.8%, which can maintain a more stable beam in the axial direction from 5.25–7.94 GHz. In addition, the maximum radiation gain at 7.1 GHz is 11.7 dBi.

4. Experimental Validation

The improved SSPPs endfire antenna was made and verified by experiments shown in Fig. 8. The vector network analyzer was used to measure the reflection coefficient, and the radiation mode was measured by the robotic

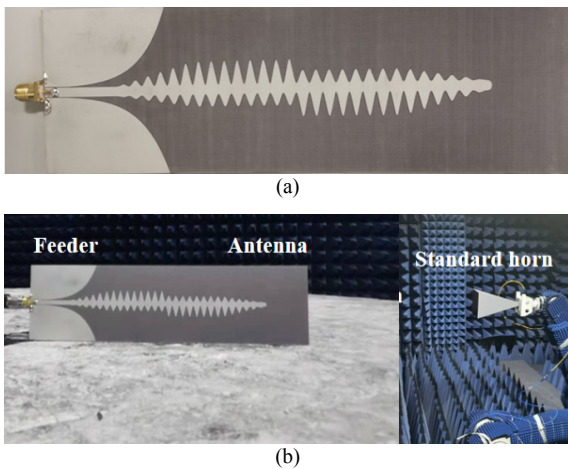


Fig. 8. (a) Photograph of the fabricated antenna. (b) Measurement setup.

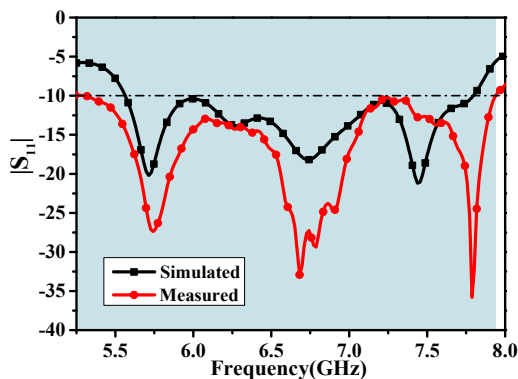


Fig. 9. Measured and simulated reflection responses of the improved antenna.

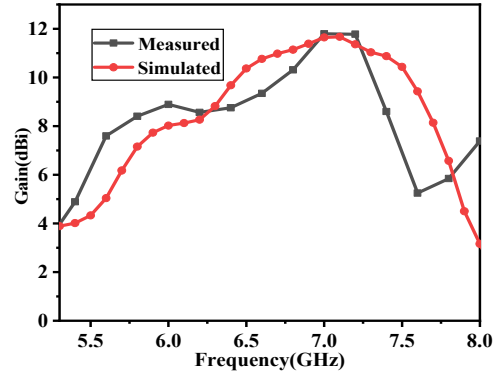


Fig. 10. Measured and simulated gain of the improved SSPPs antenna.

Ref.	Type	Length [λ_0]	Gain [dBi]	f_0 [GHz]	BW
[8]	Leaky-wave	6.0	-2-10.8	5	20%
[9]	SIW-based	3.5	7.0-11.8	3.95	8.4%
[10]	Log-periodic	2.3	6-10.9	30.5	62%
[11]	Microstrip Yagi-Uda	1.7	7.2-8.9	5.0	8%
[5]	Double SSPPs	2.3	7.0-7.1	6.1	3%
[12]	Double SSPPs	3.3	2.7-7.8	5.5	7%
[13]	Double SSPPs	5.0	8.5-15.5	24.75	23%
[14]	Single SSPPs	2.9	7.5-9.2	8.0	12%
[15]	Single SSPPs	3.7	7.1-9.0	5.05	8%
[16]	Single SSPPs	4.8	8.5-10.7	14.0	14%
Ours	Single SSPPs	4.0	7.2-11.7	6.5	40.8%

Tab. 1. Comparison of performance parameters of the same type of endfire antenna

arm. In Fig. 9, the experimental results agree well with the simulation results of the reflection coefficient, and S_{11} are suppressed below -10 dB within the operating bandwidth. The frequency offset at the resonant frequency points may be caused by fabrication errors and different relative permittivity of the substrate, but the general trend remains consistent. Figure 10 plots the relationship between the gain and frequency, showing that peak gains between 4.0 dBi and 11.7 dBi and 11.7 dBi can be achieved at 7.1 GHz. Figure 11 shows the normalized radiation pattern of the antenna at the frequency points of 5.3 GHz, 7.1 GHz, and 7.9 GHz. Good directionality is shown throughout the frequency band.

Table 1 compares other types of endfire antennas with the proposed SSPPs antenna, where f_0 represents the center frequency of the bandwidth, and λ_0 is the wavelength corresponding to the center frequency in free space. The gain of leaky wave antenna fluctuates greatly and is unstable.

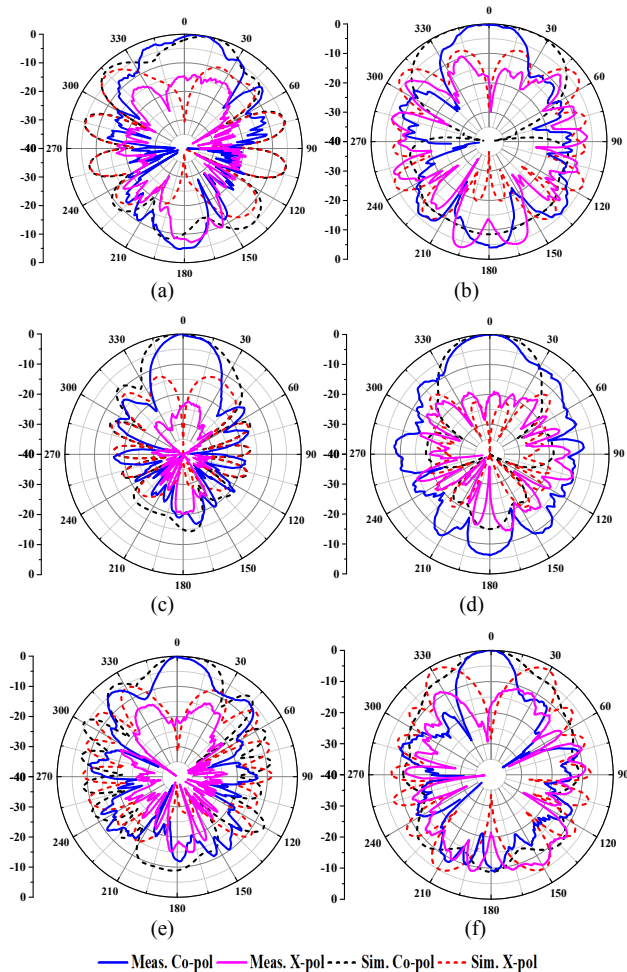


Fig. 11. Simulated and measured normalized radiation patterns. (a) xoy -plane pattern at 5.3 GHz. (b) xoz -plane pattern at 5.3 GHz. (c) xoy -plane pattern at 7.1 GHz. (d) xoz -plane pattern at 7.1 GHz. (e) xoy -plane pattern at 7.9 GHz. (f) xoz -plane pattern at 7.9 GHz.

The relative bandwidth of SIW-based antenna and microstrip Yagi-Uda antenna is very narrow. Log periodic antennas usually have high sidelobes and complex structure. Single-layer SSPPs antenna provides a new way to achieve high gain and endfire radiation. It should be noted that the single-layer SSPPs antenna requires a larger geometric size for transition, but the specific transition structure is not required in the SSPPs circuit system. Double-layer SSPPs antennas are easier to realize endfire effect than single-layer SSPPs since they are equivalent to electric dipoles but have a narrower bandwidth. Although the antenna we designed is a single-layer structure, it still achieves higher gain and wider bandwidth, and can maintain good gain. What's more, the effect is even better than the general double-layer structure, and one of the most competitive features of the antenna is that its relative bandwidth can reach 40.8%.

5. Conclusion

This paper proposes a high-gain single-layer broadband endfire antenna with high gain and directional

stability based on spoof surface plasmon polaritons. Firstly, the endfire antenna based on the basic structure of asymmetric SSPP is presented, and the field analysis is carried out. Then, an improved antenna with good directivity and broaden bandwidth is proposed. By comparing their electric field and far-field direction patterns, the theoretical basis of the antenna design was analyzed and verified through experiments. The experimental results closely follow the simulations. Finally, the improved antenna was designed to generate endfire effect in the range of 5.25–7.94 GHz with a peak gain of 11.7 dBi. The antenna can achieve good endfire performance. A great potential is demonstrated with corresponding advantages in wireless communications.

Acknowledgments

This work is supported by the National Natural Science Foundation of China (Grant No. 6217012409, 61801508), the Postdoctoral Innovative Talents Support Program of China (Grant No. BX20180375), the Natural Science Basic Research Program of Shaanxi Province, China (Grant No. 2020JM-350), the Young Talents Support Program of Shaanxi Province, China (Grant No. 20200108, No. 20210110), China Postdoctoral Science Foundation (Grant No. 2019M653960) and Young Innovation Team at Colleges of Shaanxi Province, China (Grant No. 2020022).

References

- [1] BARNES, W. L., DEREUX, A., EBBESEN, T. W. Surface plasmon subwavelength optics. *Nature*, 2003, vol. 424, no. 6950, p. 824–830. DOI: 10.1038/nature01937
- [2] TARASOV, Y. V., IAKUSHEV, D. A., USATENKO, O. V. Plasmon-polariton excitations on surfaces with fluctuating impedance. In *The 2016 9th International Kharkiv Symposium on Physics and Engineering of Microwaves, Millimeter and Submillimeter Waves (MSMW)*. 2016, p. 1–4. DOI: 10.1109/MSMW.2016.7538190
- [3] JAISWAL, R. K., PANDIT, N., PATHAK, N. P. Spoof surface plasmon polaritons based reconfigurable band-pass filter. *IEEE Photonics Technology Letters*, 2018, vol. 31, no. 3, p. 218–221. DOI: 10.1109/LPT.2018.2889007
- [4] WEI, D., LI, J., YANG, J., et al. Wide-scanning-angle leaky-wave array antenna based on microstrip SSPPs-TL. *IEEE Antennas and Wireless Propagation Letters*, 2018, vol. 17, no. 8, p. 1566–1570. DOI: 10.1109/LAWP.2018.2855178
- [5] YIN, J., BAO, D., REN, J., et al. Endfire radiations of spoof surface plasmon polaritons. *IEEE Antennas and Wireless Propagation Letters*, 2017, vol. 16, p. 597–600. DOI: 10.1109/LAWP.2016.2592512
- [6] LI, S., ZHANG, Q., XU, Z., et al. Phase transforming based on asymmetric spoof surface plasmon polariton for endfire antenna with sum and difference beams. *IEEE Transactions on Antennas and Propagation*, 2020, vol. 68, no. 9, p. 6602–6613. DOI: 10.1109/TAP.2020.2993083
- [7] LIU, L., CHEN, M., YIN, X. Single-layer high gain endfire antenna based on spoof surface plasmon polaritons. *IEEE Access*, 2020,

vol. 8, p. 64139–64144. DOI: 10.1109/ACCESS.2020.2984153

- [8] LIU, P., FENG, H., LI, Y., et al. Low-profile endfire leaky-wave antenna with air media. *IEEE Transactions on Antennas and Propagation*, 2018, vol. 66, no. 3, p. 1086–1092. DOI: 10.1109/TAP.2018.2790042
- [9] ZHAO, Y., SHEN, Z., WU, W. Wideband and low-profile H-plane ridged SIW horn antenna mounted on a large conducting plane. *IEEE Transaction on Antennas and Propagation*, 2014, vol. 62, no. 11, p. 5895–5900. DOI: 10.1109/TAP.2014.2354420
- [10] ZHAI, G., CHENG, Y., YIN, Q., et al. Gain enhancement of printed log-periodic dipole array antenna using director cell. *IEEE Transactions on Antennas and Propagation*, 2014, vol. 62, no. 11, p. 5915–5919. DOI: 10.1109/TAP.2014.2355851
- [11] SHI, J., ZHU, L., LIU, N. W., et al. A microstrip Yagi antenna with an enlarged beam tilt angle via a slot-loaded patch reflector and pin-loaded patch directors. *IEEE Antennas Wireless and Propagation Letters*, 2019, vol. 18, no. 4, p. 679–683. DOI: 10.1109/LAWP.2019.2901033
- [12] TIAN, D., XU, R., PENG, G., et al. Low profile high-efficiency bidirectional endfire antenna based on spoof surface plasmon polaritons. *IEEE Antennas and Wireless Propagation Letters*, 2018, vol. 17, no. 5, p. 837–840. DOI: 10.1109/LAWP.2018.2818109
- [13] ZHANG, X.-F., SUN, W. J., CHEN, J. X. Millimeter-wave ATS antenna with wideband-enhanced endfire gain based on coplanar plasmonic structures. *IEEE Antennas and Wireless Propagation Letters*, 2019, vol. 18, no. 5, p. 826–830. DOI: 10.1109/LAWP.2019.2902874
- [14] KANDWAL, A., ZHANG, Q., TANG, X. L., et al. Low-profile spoof surface plasmon polaritons traveling-wave antenna for near-endfire radiation. *IEEE Antennas and Wireless Propagation Letters*, 2018, vol. 17, no. 2, p. 184–187. DOI: 10.1109/LAWP.2017.2779455
- [15] ZHUANG, K., GENG, J., WANG, K., et al. Pattern reconfigurable antenna applying spoof surface plasmon polaritons for wide angle beam steering. *IEEE Access*, 2019, vol. 7, p. 15444–15451. DOI: 10.1109/ACCESS.2019.2895106
- [16] GE, S., ZHANG, Q., RASHID, A. K., et al. Analysis of asymmetrically corrugated Goubau-line antenna for endfire radiation. *IEEE Transactions on Antennas and Propagation*, 2019, vol. 67, no. 11, p. 7133–7138. DOI: 10.1109/TAP.2019.2927633

About the Authors ...

Huan JIANG was born in Sichuan province, China. He received his B.S. degree from the Air Force Engineering University (AFEU) in 2020. He currently works towards his M.S. degree. His research interests are in antennas design, antenna array design and their applications.

Xiang-yu CAO (corresponding author) received her M.S. degree from Air Force Missile Institute in 1989. In the same year, she joined the Air Force Missile Institute. She received her Ph.D. degree from the Missile Institute of AFEU in 1999. From 1999 to 2002, she was engaged in postdoctoral research at Xidian University, China. She was a Senior Research Associate in the Department of Electronic Engineering, City University of Hong Kong from June 2002 to Dec. 2003. She is currently a Professor and a senior member of IEEE. Her research interests include computational electromagnetics, electromagnetic metamaterials and their antenna applications.

Huan-huan YANG (Member, IEEE) received the M.S. and Ph.D. degrees from the Air Force Engineering University (AFEU), Xi'an, China, in 2012 and 2016, respectively. He was a Joint-Supervision Ph.D. Student with AFEU and also with Tsinghua University, Beijing, China. He is currently a Lecturer and also a Post-Doctoral Researcher with AFEU. He has authored or coauthored more than 50 technical articles. His research interests include advanced antenna array, reconfigurable antenna, reflectarray, metasurface, and radar cross section (RCS) reduction technique. Dr. Yang was a recipient of the Postdoctoral Innovative Talents Support Program of China. He has served as the Session Chair and a TPC Member for the International Applied Computational Electromagnetics Society (ACES) in 2018 and 2019, respectively.

Jun GAO received the B.Sc and M.A.Sc degrees from the Air Force the Missile Institute in 1984 and 1987, respectively. He joined the Air Force Missile Institute in 1987 as an Assistant Teacher. He became an Associate Professor in 2000. He is currently a Professor of the Information and Navigation College, Air Force Engineering University of CPLA. He has authored and coauthored more than 100 technical journal articles and conference papers, and holds one China soft patent. His research interests include smart antennas, electromagnetic metamaterial and their antenna applications.

Liao-ri JI-DI was born in Sichuan province, China. He received his B.S. degree from the Electronic and Information College, Tongji University in 2016, and he was the commencement student speaker of Tongji University in 2016. He currently works towards his M.S. degree. In his research, he specializes in metamaterial, antenna array design and RCS reduction techniques.